Crystallization process of transparent conductive oxides $Zn_kIn_2O_{k+3}$

Toshihiro Moriga,[a*] Akihiko Fukushima,[a] Yozo Tominari,[a] Shoji Hosokawa,[a] Ichiro Nakabayashi,[a] and Kikuo Tominaga[b]

[a]Department of Chemical Science and Technology, Faculty of Engineering, The University of Tokushima, 2-1 Minami-Josanjima, Tokushima 770-8506, Japan, [b]Department of Electric and Electronic Engineering, Faculty of Engineering, The University of Tokushima, 2-1 Minami-Josanjima, Tokushima 770-8506, Japan.
Email:moriga@chem.tokushima-u.ac.jp

Crystallization process of the homologous compounds $Zn_kIn_2O_{k+3}$ from the coprecipitants was examined by XAFS spectroscopy and X-ray diffractometry. Interesting crystallization behavior could be observed. Though zinc oxide already crystallized as the wurtzite-type ZnO at 573K, indium oxide remained amorphous. Subsequently bixbyite-type In_2O_3 appeared at 873K for k=5 and 7 and at below 773K for the other k-members, respectively. The In-O distance in the amorphous In_2O_3 was a little shorted than that in the bixbyite-type In_2O_3 by 0.06-7Å. The distance remained constant but abruptly increased to that observed in the bixbyite-type In_2O_3 in accordance with the progress of crystallization. Then the distance gradually decreased and converged to *ca*. 2.12Å at the temperature range of 1173-1373K, due to the reaction between In_2O_3 and ZnO to form the homologous compound.

Keywords: homologous compounds, crystallization process, transparent conductive oxides

1. Introduction

Transparent conductive oxides, or TCOs, are widely used as transparent electrodes for flat panel displays and solar cells. Commercial, thin-film tin-doped indium oxide, or ITO, exhibits a conductivity of 1000-5000S/cm and an optical transparency of 85-90%. Nevertheless, alternative materials with higher conductivity, better transparency at blue-green wavelengths and lower cost are desired. There have been several recent reports of TCOs in the ZnO-In_2O_3 system, demonstrating that high transparency and high conductivity can be achieved (Minami *et al.*, 1996, Phillips et al., 1994, Moriga *et al.*, 2000). We have reported that amorphous oxide films with a [In]/([Zn]+[In]) ratio of *ca*. 0.25 deposited at 423K showed the maximum conductivity more than 4000S/cm and maximum carrier concentration of $1.2\times10^{21}cm^{-3}$.

ZnO and In_2O_3 react at high temperatures (>1273K) to form a series of homologous compounds, $Zn_kIn_2O_{k+3}$, where k is an integer (Moriga *et al.*, 1998). We have examined equilibrium phase relationships in the ZnO-In_2O_3 system between 1373 and 1673K using solid state reaction technique and X-ray diffractometry. Nine homologous compounds with k=3, 4, 5, 6, 7, 9, 11, 13, and 15 were observed and $Zn_5In_2O_8$ (k=5) and $Zn_7In_2O_{10}$ (k=7) were the most stable to form the homologous compounds at the temperature as low as 1373K.

Generally, amorphous oxides can easily be obtained by sol-gel method such as coprecipitation method. However, no structural technique at present can uniquely describe the structure of amorphous solid. This is because of the loss of the periodicity in disordered materials. Therefore the structure of such materials can only be described in terms of mean values of distance, coordination number, Debye-Waller factor obtained by XAFS. In this study, we examined the local structures of amorphous $Zn_kIn_2O_{k+3}$ obtained by coprecipitation method by means of XAFS, and found that the manners of crystallization differ between the two stable homologous compounds and the others.

2. Experimental

A series of compositions (k=3, 5, 7, 9, 11, and 15 in $Zn_kIn_2O_{k+3}$) were prepared by the aqueous solutions of $Zn(NO_3)_2\bullet6H_2O$ and $In(NO_3)_3\bullet3H_2O$ (>99% purity, on a cation basis, Kishida Chemicals, Japan). Diethylamine was added to the mixed solutions to form a sol of metallic hydroxide. After washing with acetone, the coprecipitant was dried at 373K in air for 24h, and fired at the several temperatures of 573-1373K in air for 24h in high-density alumina crucibles. The crystallization temperature for each sample was confirmed by X-ray diffraction technique.

X-ray absorption spectra near In K-edges were measured at BL-10B branch line with Si(311) channel-cut monochromator in the Photon Factory, KEK, Japan. The storage ring was operated at 3.0GeVwith a typical current of 100mA. The peak position at the midpoint of the Cu K-edge jump for Cu foil was calibrated to be 12.7190º. All the measurements were performed in a transmission mode at room temperature.

Using the program library "XANADU" (Sakane *et al.*, 1993), the EXAFS data analyses were performed. Background was calculated by a least-squares fitting of the pre-edge region with Victoreen's formula. The energy of the mid-point of the edge jump was used as the value of the threshold energy (E_0). At the Fourier transform calculation of EXAFS, Hanning window function was used to reduce ripples in the transform. The phase shift and the backscattering amplitude function used were the theoretical values tabulated by Teo and Lee (Teo & Lee, 1979) or McKale *et al*. (McKale *et al*., 1988), combined with interpolation using a natural cubic spline function. The same k-range of $3.5Å^{-1}\leq k\leq13.5Å^{-1}$ for In K-edge was used for the transform. In Fourier filtering, the smooth window function was used. The r_{min}, r^s_{min}, r^s_{max} and r_{max} were typically 1.56Å, 1.68Å, 2.51Å and 2.65Å. Here the r_{min} and the r_{max} are the limits in the r-space for the transform and the r^s_{min} and r^s_{max} are the square window limit. In order to determine structural parameters of the first shell around In, a curve-fitting technique was applied. In the curve-fitting, each coordination shell has its own scattering atom (oxygen), interatomic distance *r*, amplitude factor B, *k*-dependent mean-free path of photoelectron η (=k/λ), Debye-Waller-type factor σ and energetic difference ΔE_0 between the experimentally determined E_0 and the theoretical one. The amplitude factor B is in proportion to coordination number (CN). The cubic bixbyite-type In_2O_3 (CN=6, r=2.17Å in average) (Marezio, 1966) were used for reference of amplitude factor B. The amplitude factor obtained by the analysis was converted into CN. The same- k-range of $5Å^{-1}<k<13Å^{-1}$ was used for the curve-fitting. The errors estimated can be as small as $\leq$0.01Å in distance and $\leq$1 CN, according to the method suggested at the "International Workshop on Standards and Criteria in X-ray Absorption Spectroscopy 1988" (Lytle *et al.*, 1989).

3. Results and Discussions

Figure 1 shows the composition dependence of X-ray diffraction patterns of $Zn_kIn_2O_{k+3}$ precursors (k=3, 5, 7, 9, 11 and 15) fired at 773K. For specimens fired at 573K, only the peaks assigned to the wurtzite-type ZnO could be observed. The lattice parameters for all the specimens were a=3.248$\pm$0.005Å and c=5.20$\pm$0.01Å, which are in a good agreement with those of ZnO reported in the JCPDS file (Card No.36-1451, a=3.2498Å and c=5.2066Å),

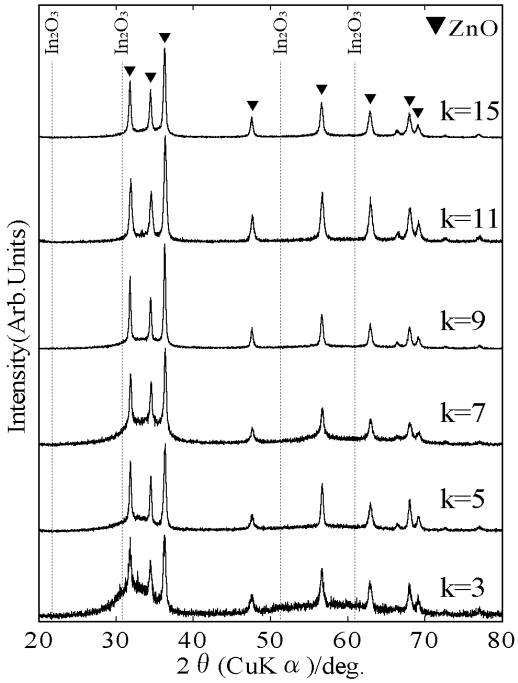

Figure 1
Composition dependence of X-ray diffraction patterns of $Zn_kIn_2O_{k+3}$ precursors (k=3, 5, 7, 9, 11 and 15) fired at 773K.

suggesting that indium is not occluded into the wurtzite-type ZnO matrix. The indium is considered to exist as an amorphous In_2O_3. For specimens fired at 773K as shown in Fig. 1, two types of diffraction patterns were observed. For the compositions of k=5 and 7, the feature of diffraction patterns did not change. For the other compositions, the amorphous In_2O_3 crystallized to form the bixbyite-type In_2O_3. The peak positions of the wurtzite-type ZnO did not change. These phenomena imply that the crystallization of the amorphous In_2O_3 in the specimens of k=5 and 7 fired at 773K was inhibited. The reason why the crystallization of In_2O_3 in these specimens should be inhibited is not clear. However, the corresponding compositions of these specimens would form the homologous compounds $Zn_5In_2O_8$ and $Zn_7In_2O_{10}$ when heated at higher temperature. The two homologous compounds form more

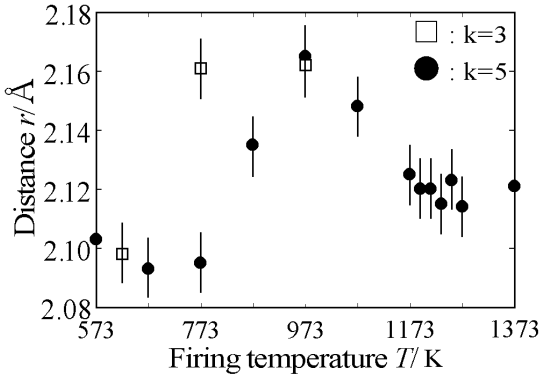

Figure 2
Variation of In-O distance of $Zn_5In_2O_8$ (k=5) and $Zn_3In_2O_6$ (k=3) precursors determined by curve-fitting technique of In K-EXAFS spectrum, as a function of firing temperature.

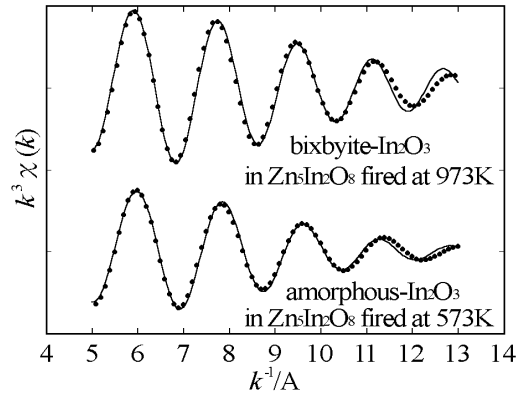

Figure 3
K-edge experimental (solid line) and calculated (dotted line) k^3-weighted EXAFS signals for the $Zn_5In_2O_8$ precursors fired at 573 and 973K.

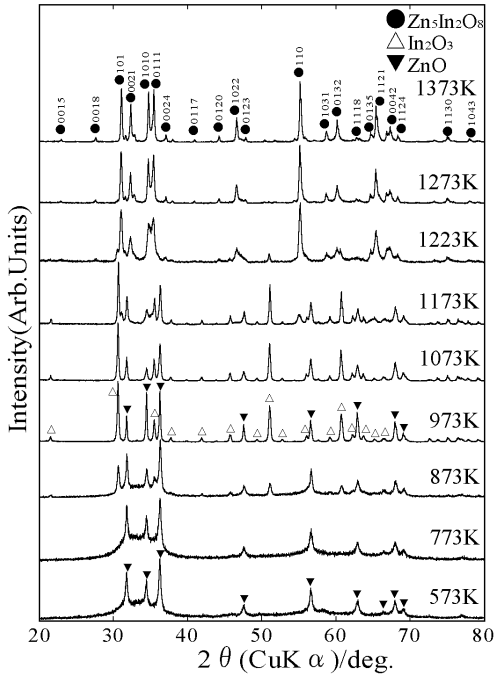

Figure 4
Variation of X-ray diffraction patterns of $Zn_5In_2O_8$ precursors as a function of firing temperature.

easily than any other compounds. It is possible that the fact would concern with the inhibition of crystallization.

Figure 2 shows variation of In-O distance of the $Zn_5In_2O_8$ (k=5) precursors determined by curve-fitting technique of In K-EXAFS spectrum, as a function of fired temperatures. The distances of the $Zn_3In_2O_6$ (k=3) precursor fired at 623, 773 and 973K are also shown for references. Samples of In K-edge experimental and calculated k^3-weighted EXAFS signals for the $Zn_5In_2O_8$ precursors fired at 573 and 973K are shown in Fig. 3. For specimens with k=5, the In-O distances of the amorphous In_2O_3 remained constant in a temperature range of 573-773K, which are

Table 1
Results of curve-fitting analysis for the first In-O shell of $Zn_5In_2O_8$ precursors. Note that η value was fixed at 2.54Å when the precursors were analyzed.

Fired temp. [k]	r/Å	CN	η/Å	σ/Å^{-1}	ΔE_0/eV	R/%
In_2O_3 (ref.)	2.170	6	2.54	0.06	9.53	8.99
573	2.102	5.0	-	0.10	6.85	11.98
673	2.093	5.0	-	0.10	7.42	11.42
773	2.095	4.9	-	0.09	6.66	12.50
873	2.137	5.6	-	0.09	7.10	13.72
973	2.164	6.2	-	0.07	8.59	10.92
1073	2.151	5.8	-	0.06	7.68	10.37
1173	2.123	5.7	-	0.06	7.24	9.96
1273	2.116	5.7	-	0.07	7.31	10.75
1373	2.120	5.8	-	0.06	7.96	9.84

calculated to be 2.09-2.11Å. The distance corresponds to the intermediate value between sum of the effective ionic radii of the 6-fold In^{3+} ion and O^{2-} ion and that of the 5-fold In^{3+} ion and O^{2-} ion. The In^{3+}-O^{2-} bond distance can be calculated to be 2.09Å when the coordination number of In^{3+} is 5 and to be 2.18Å when the number of In^{3+} is 6. The In-O distance in the amorphous In_2O_3 was a little shorter than that in the bixbyite-type In_2O_3 by 0.06-7Å. The feature of XANES spectrum for the amorphous In_2O_3 was, however, identical with that for the bixbyite-type In_2O_3. These facts indicated that the local structure of the amorphous In_2O_3 would fundamentally be the same as the bixbyite-type In_2O_3. The CN obtained for the amorphous samples were *ca*. 20% smaller than that obtained for the bixbyite-type In_2O_3. As some parts of oxygen are missing, periodicity of the ion arrangements is so poor that the In_2O_3 should exist as an amorphous solid. For specimens with k=3, the In-O distance increased to be 2.16Å at 773K, as amorphous In_2O_3 crystallizes at 773K.

The increase of In-O distances in $Zn_5In_2O_8$ precursor from 773K up to 973K is due to the crystallization of In_2O_3, which was confirmed by X-ray diffraction as shown in Fig. 4. Then the distance gradually decreased and converged to *ca*. 2.12Å at the temperature range of 1173-1373K. This results from the reaction between In_2O_3 and ZnO to form the homologous compound $Zn_5In_2O_8$. The reaction seemed to begin at around 1073K and to complete at 1223-1273K by X-ray diffraction. In ions in $Zn_5In_2O_8$ occupy both the 6-fold octahedral site in the InO_2^- layers and the 5-fold trigonal bipyramid site in the $(InZn_5)O_6^+$ layers (Kimizuka *et al*., 1994), so that the observed distance by XAFS at 1173-1373K converged to intermediate value between the 6-fold In^{3+} ion and the 5-fold In^{3+} ion.

In the Fourier transforms of In K-EXAFS spectra of the $Zn_5In_2O_8$ precursor as a function of fired temperatures shown in Fig. 4, only one major peak is present for the amorphous In_2O_3 fired at 573-773K. It suggests that only the first coordination shell contributes mainly to the EXAFS signal. Outer shells cannot be observed due to large disorder in an amorphous solid (Dalba *et al.*, 1993). When the firing temperature rises, the amorphous In_2O_3 reacts to crystallize into $Zn_5In_2O_8$ through the bixbyite-type In_2O_3, so that the second or third major peaks due to the second shell constituting In-In pairs grows around 3-4Å in the radial distribution function. The fact that only one peak is present in the Fourier transform of an EXAFS spectrum is a good indication of the amorphous nature of the sample measured.

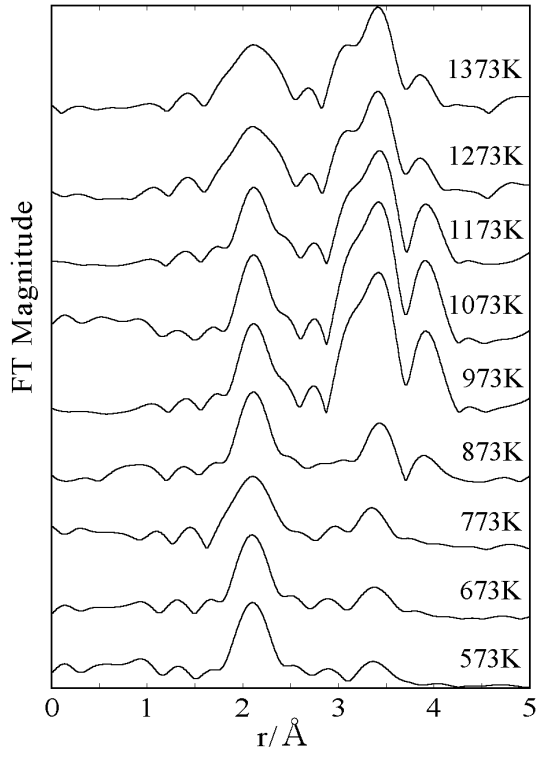

Figure 5
Fourier transforms of In K-EXAFS spectra of $Zn_5In_2O_8$ precursors as a function of firing temperature.

XAFS experiments were performed under the approvals of the Photon factory Program Advisory Committee (Proposal Nos. 97G029 and 99G064).

References

Dalba, G., Fornasini, P., Diop, D., Grazioli, M., & Rocca, F. (1993) *J. Non-Cryst. Solids* **164-166**, 159-162.
Lytle, F. W., Sayer, D. E., & Stern, E. A. (1989) *Physica B* **158**, 701-722.
Kimizuka, N., Isobe, M., & Nakamura, M. (1994) *J. Solid State Chem.* **116**, 170-178.
Marezio, M. (1966) *Acta Crystallogr*. **20**, 723-728.
McKale, A. G., Veal, B. W., Pailikas, A. P., Chan, S. K. & Knapp, G. S. (1988) *J. Am. Chem. Soc.* **110**, 3763-3768.
Minami, T., Kakumu, T., & Tanaka, S. (1996) *J. Vac. Sci. Technol. A* **14**, 1704-1708.
Moriga, T., Edwards, D. D., Mason, T. O., Palmer, G. B., Poeppelmeier, K. R., Schindler, J. L., Kannewurf, C. R., & Nakabayashi, I. (1998) *J. Am. Ceram. Soc.* **81**, 1310-1316.
Moriga, T., Okamoto, T., Hiruta, K., Fujiwara, A., Nakabayashi, I., & Tominaga, K. (2000) *J. Solid State Chem.*, in press.
Sakane, H., Miyanaga, T., Watanabe, I., Matsubayashi, N., Ikeda, S., & Yokoyama, Y. (1993) *Jpn. J. Appl. Phys.* **32**, 4641-4647.
Teo, B. K., & Lee, P. A. (1979) *J. Am. Chem. Soc.* **101**, 2815-2832.

Received 31 July 2000 • Accepted 22 November 2000